Journal of Materials and Applications 2020;9(2):107-119
https://doi.org/10.32732/jma.2020.9.2.107

Enhanced Luminescence of Silver Nano-particles Doped Na_2O-BaO-Borate Glasses

Rajeshree Patwari D[1], B Eraiah[2]

1. Department of Physics, Government Science College, Bangalore-560001, Karnataka, India
2. Department of Physics, Bangalore University, Bengaluru-560056, Karnataka, India
E-mail: eraiah@rediffmail.com

Received: 9 August 2020; Accepted: 9 September 2020; Available online: 15 October 2020

Abstract: Na_2O-BaO-Borate glasses were synthesized with silver nano-particles of varying silver concentrations by the method of melt-quenching. Their densities of the glasses and hence molar volumes were computed. The existence of the silver nano-particles was depicted by characteristic band in the absorption spectra of UV- Visible studies known as plasmon band. Further the matrix also showed a small amount of nanostructures of the host which imparts the nonlinear behaviour. They were further visualized by the Scanning and Transmission electron microscopy. Optical band gap and Urbach energies were found. The band gap values change exactly in the opposite manner of density with silver doping. The wide luminescence band in the visible region formed for the excitation of plasmon band may be utilized for the luminescence enhancement of luminescent material like rare earth ions. The very significant result perceived from this is that the glass as such with silver nano-particles showed broad emission in the, green & blue portions of electromagnetic spectrum in the close vicinity of white light with the variation of silver content which can be utilized for the enrichment of the emission of lanthanide ions in the visible section of electro-magnetic spectrum.
Keywords: Band gap energy; Silver nanoparticles; Surface plasmon resonance.

1. Introduction

Glass is a very vital material both in the ancient times as well as in the present scenario. Materials are used in the form of glass from scientific laboratories equipments to more sophisticated instruments in the medical field. The significance of glasses lies in its ease of formation as well as it can tailored into any desired shapes like sheets, glass wools, rods, thin films, fibers etc. Glass as such is highly transparent dielectric material and mainly attracted by its beautiful colours and its vast application. It is a very good material especially for accomodating the impurities to impart the desired structural[1], optical[1,2], mechanical[3], conducting[4] and magnetic properties[5]. Though wide applications of silica glasses are satisfactory, the borate glasses are also receiving more attention due to their low cost, low melting point and ease of glass forming[6]. Borate glasses are attracting more interest due to their optical and electro-chemical applications such as luminescent, optical waveguides materials, solid-state batteries [7]. Most of the studies on borate glasses were conducted on their structural,optical, magnetic and electrical studies [8-10].

It was planned for the creation of silver nano-particles in the glass host. As less work was done with silver nanoparticles in borate glasse despite of its many desired qualities.For this purpose we chose the borate glasses as a result of its numerous beneficial properties like lower melting temperature, higher transparency, higher ability to form glass, higher solubility of rare earth. Barium oxide, one of the heavy metal like TeO_2, Bi_2O_3, PbO metal utilized as a modifier and it grants nonlinear behavoiur to the glass. Sodium oxide is likewise utilized as a modifier which decreases the melting temperature and additionally works as electron rich centre apart from acting as a reducing agent.

The present work was focussed on synthesizing strong glasses with silver nano-particles both chemically and physically stable. And to achieve this, we attempted glasses with above said chemicals with different variations of silver nitrate. The preparation of the borate glasses, modified by barium oxide and sodium oxide, with silver nanoparticles was done successfully by utilising the melt quenching method. The investigations of these glasses in relation to their physical, molecular-structural, optical absorption and luminescence properties were made with the aid of many sophisticated instruments which are discussed. Silver nitrate showed very good solubility than the silver chloride.The silver nanoprticles generated were studied with spectrometric techniquices.The Plasmon behaviour of the silver nanopaticles were tried to use for the enhancement of luminescence which may be further

used for the rare earth luminescence boosting when the glasses were doped with both silver nanoprticles and the lanthanide ions.

2. Experimental procedure

Sodium-barium-borate glasses with varying silver nitrate content were prepared by the traditional melt-quenching procedure. The chemicals used for the preparation were all analytical grade. The chemicals used were boric acid (H_3BO_3), barium carbonate ($BaCO_3$), sodium carbonate ($Na_2CO_{3)}$ and silver nitrate ($AgNO_{3)}$.

Required quantities of the chemicals according to the stoichiometry were weighed with the electronic balance. The mixture was powdered and blended well for uniform distribution of all the involved materials. And this solid mixture was placed into a Muffle furnace and heated till a clear molten liquid is formed with frequent stirring. After ensuring no air bubbles, at 1000^{o}C the melt was immediately poured between the two preheated brass moulds to prepare the glasses. Since these glasses were very delicate, they were kept for annealing for two hours without any delay at 300^{o}C and then naturally cooled to room temperature. The annealing is needed to reduce the strain developed due to the sudden cooling the melt and the glass also become tough after annealing. With the help of emery papers of different grade 100-1200 the glasses were polished starting with lower value to higher and used for different studies. Archimedes procedure was employed to evaluate the density of these glasses and then molar volume was determined. Structural studies were worked out by P.X-ray diffraction (Powdered XRD), fourier-transform infra-red spectroscopy (FTIR) and Raman spectroscopy (RS). The size, shape of nanoparticles and their distribution were analysed by microscopic techniques, scanning - electron microscopy (SEM) and transmission - electron microscopy (TEM). Optical absorption and luminescence studies were carried out by UV-Visible absorption and spectro-fluoremeter respectively.

3. Results and discussions

The different chemical and their stoichiometric molar compositions of the glasses prepared are shown in the table 1.

Table 1. The chemical composition of borate glasses with different silver concentration

Glass Code	B_2O_3	BaO	Na_2O	AgO
B-0	60	10	30	0.0
BA-0.25	59.75	10	30	0.25
BA-0.5	59.50	10	30	0.5
BA-0.75	59.25	10	30	0.75
BA-1.0	59	10	30	1.0
BA-1.25	58.75	10	30	1.25

The BaO and Na_2O modified borate glasses were prepared with varying molar concentrations of silver oxide of 0.0, 0.25, 0.5, 0.75, 1.0 1nd 1.25mol%. All the materials involved for the preparation of glass were of analytical grade. Borates from boric acid were used for glass network because of their higher affinity towards glass forming. Lead oxide (PbO), the most commonly used but more toxic heavy metal oxide was replaced by the barium oxide which acts as modifier and imparts non-linear properties to the glass as well. The alkali oxide, Na_2O is another modifier. It decreases the hygroscopic nature of the borate glass and helps in the reduction silver ions. Silver oxide from silver nitrate is used for the formation and growth of silver nanoparticles.

3.1 Physical appearance

The glasses prepared were observed to be strong, stable, and highly transparent. The glasses without silver were white transparent. The silver doping gave slight yellow colouration, which increased with the silver content increase in the glass and the glasses were also transparent. These are named as silver doped borate glasses or simply BA-glasses with varying silver concentration from 0 to 1.25 with a step size of 0.25.

3.2 Density and molar volume

Using the Archimedes principle the densities of the prepared BA glasses with varying silver doping were found by measuring the weight of the glass in air and in toluene, which were taken for immersing the sample.

The density of the samples was computed using the equation

$$\rho_{\text{glass}} = \rho_{\text{toluene}} \left(\text{Wt}_{\text{air}}/\text{loss of Wt}_{\text{toluene}}\right) \quad (1)$$

The molar volueme of the glasses was calculated using the formula

$$M_v = M_m/\rho_{glass} \quad (2)$$

where M_m- molar mass of the glass

The densities and the molar voluemes were plotted (Fig. 1). With the increase in silver doping the density of BA glasses initially increased and then started decreasing with further silver content increase, in the glass. However, the molar volume showed opposite trend as that of density. This is because initially the silver goes in the voids and interstitials with more addition of silver may be volume is increased in order to accommodate the increased silver doping hence density is decreasing and the molar volume in increasing with the silver concentration.

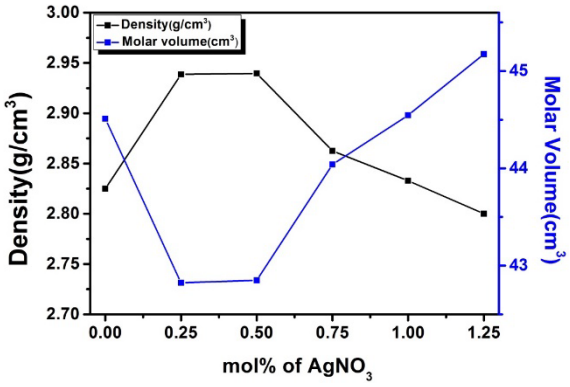

Figure 1. The variation of density and molar volume of the BA- glasses with the concentration of silver doping

3.3 Structural properties

3.3.1 Powdered X-ray diffraction (PXRD)

The PXRD of the BA- glasses (Fig.2) showed no sharp peaks which suggested the amorphous nature of the prepared glasses [11]. This disordered arrangement of entities substantiates the amorphous nature of the samples prepared.

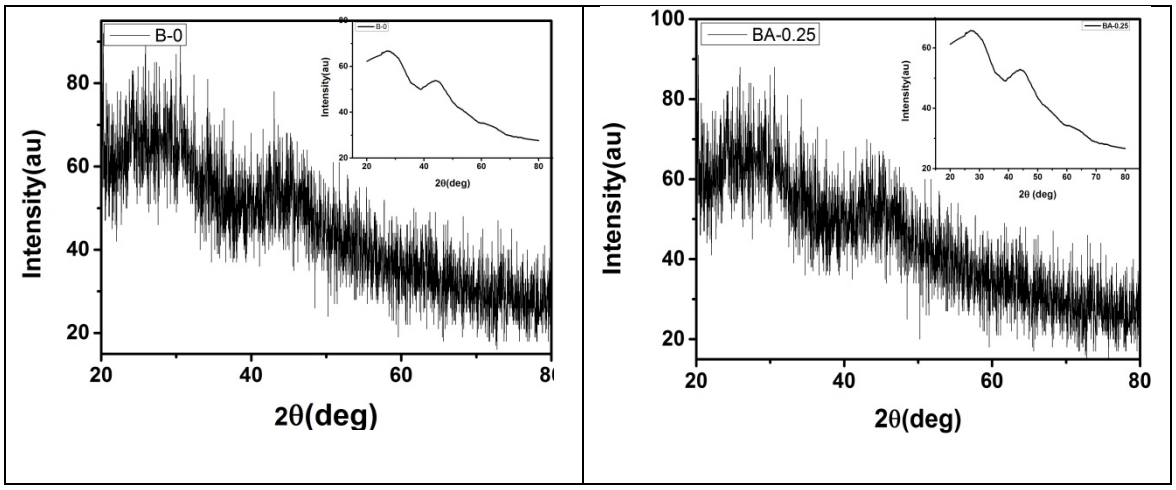

Figure 2. Powdered X-Ray diffraction spectrum of the B-0 and BA-0.25 Glasses

Table 2. The position of the two broad humps of the silver doped borate glasses

Glasses	Broad hump I	Broad hump II
B-0	24.35	43.22
BA-0.25	24.35	43.22
BA-0.5	24.35	43.22
BA-0.75	24.95	44.23
BA-1.0	25.52	44.98
BA-1.25	25.52	44.98
Average	24.84 ≅25	43.98 ≅ 44

The peak envelops are shown as insights and their peak positions after fitting the peaks are shown in the table 2. A negligible variation in the two wide peaks positions was observed. The two broad absorption humps were seen around 25° and 44° (average values) and were due to the collective scattering of all the molecules and atoms simultaneously. The lack of long range order and the absence of sharp and discrete peaks which is characteristics of systematic periodic arrangement of atoms or molecules were observed. The lack of regular repetitive positioning is also known as glass.

3.3.2 FTIR studies of the silver doped glasses

The FTIR spectra of BA- glasses were shown in the figure 3. The spectra are repetitive and all the absorption peaks of composite nature having multiple peaks overlapping on one another, because of the presence of both tetragonal and trigonal structural groups were observed. Clear examination of the spectra indicated presence of the bands of vibration due to different collection of BO_3 and BO_4 structural units. Many absorption bands were detected at 1333, 1132, 994, 944, 854, 826, 707 and 464cm^{-1} in this spectra. The trigonal BO_3 unequal stretching vibrations were observed at 1333cm^{-1} [12] in the wavenumber range 1200-1600cm^{-1}, Stretching vibrations of B-O bond in tetrahedral BO_4 group in the range 800-1200cm^{-}, BOB bending vibrations and BOBa stretching vibrations were observed.

The band identified at 707cm^{-1} revealed the B-O-B bending vibrations in the borate glass net-works [13]. The small, weaker bands near 464cm^{-1} < 600cm^{-1} can be assigned to Ba, which replaced Na in the matrix [14, 15]. The peak around 994cm $^{-1}$dipicts the stretching vibrations of the bond B-O-Ba. [15]. There were no boroxol rings in the absence of peak 800cm^{-1}. The peak 826cm^{-1} is assigned to the diborate linkage [15]. The B-0 glass showed minimum and the BA-1 glass maximum values of absorbance for all the observed peaks. The peak intensity is found to increase with silver doping and at 1.25mol% doping it showed a decrease. The least intensity of absorbance was seen in the base glass. The silver doping may be facilitating the breaking of larger borate structure into smaller ones which in turn may be responsible for the increased intensity of the doped glasses.

3.3.3 Raman studies

Raman spectroscopy was employed to study the structure of materials by their molecular vibrations by absorbing particular wavelength. Figure 4 shows the Raman spectra of the silver doped glasses. Largely small groups of triborate (BO_3) and tetraborate (BO_4) are the main constituents of the borate glasses. Based on the combinations of these two groups they are named as Boroxol ring, triborate, di-triborate with and without non-bridging oxygen atom, diborate, metaborate, pyroborate, orthoborate etc.

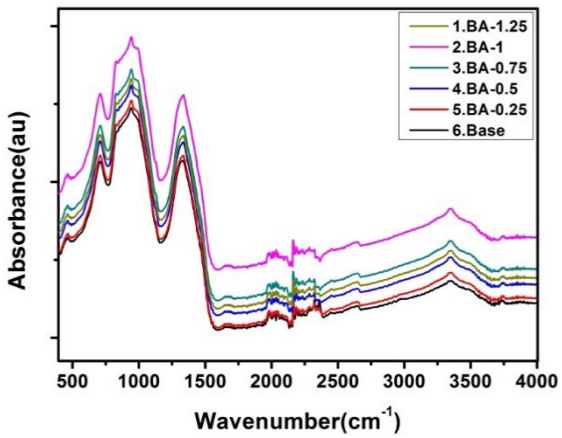

Figure 3. FTIR spectra of BA- glasses

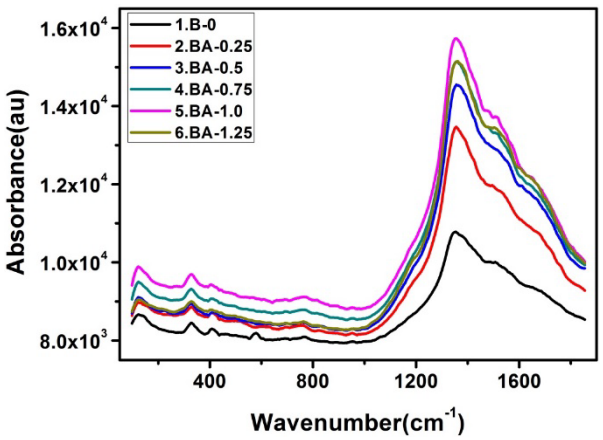

Figure 4. Raman spectra of Silver doped borate glasses

Raman Spectra show the absorption around the wave numbers 124, 157, 225, 264, 329, 407, 579, 766, 952, 1183, 1339, 1527, 1678cm^{-1}. The peak 597 cm^{-1} is more prominent only in base glass. The highest intensity peak 1339 shows shift with respect to the silver doping and also variation in intensity. Deconvoluted Raman spectra are shown in the figure 5.

Tetrahedral BO_4 was assigned to the Raman bands around 407 and 264cm^{-1}[14] in barium diborate. Comparatively wider and weak band between 950- 962cm^{-1} were attributed to asymmetric stretching of BO_3 present in barium borates [15]. The band 766cm^{-1}associated to symmetric vibrations six membered ring in which one or two triangular BO_3 groups were replaced by tetrahedral BO_4 groups[16].

The bands in the range 1300-1600cm^{-1} signify the triborate structures involving one non-bridging oxygen atom [17]. The highest frequency band between 1200-1600cm^{-1}[18] was assigned to B-O that does not belong to the

boroxol rings. The peaks formed by the presence of other metal oxides fall in the wavenumber less than 500cm^{-1} [19]. 1183cm^{-1} is assigned to the BO_3 also. The peak position and the width of the borate glasses are shown in the table 3 and table 4. The band position and the band width were found to decrease and then increased with the silver concentration. All the peaks are showing increasing intensity with silver concentration upto1.0 mol% and then it decreases with further increase of silver as depicted in the table 5. And 4th and 6th peaks showed an increase in the intensity for all concentration. First peak showed a small decrease initially and then a gradual increase in intensity with silver doping. This increase in intensity may be attributed to the silver nanoparticles whose ease of forming dipoles in the field may be facilitating the oscillation of the borate groups.

Table 3. Deconvoluted bands peak positions of Raman spectra of silver doped borate glasses

Peak No	B-0	BA-0.25	BA-0.5	BA-0.75	BA-1.0	BA-1.25
1	129	134	132	131	131	131
2	256	248	245	246	229	289
3	1234	1219	1221	1223	1225	1206
4	1353	1354	1356	1353	1351	1356
5	1461	1468	1468	1462	1455	1484
6	1602	1583	1589	1597	1610	1582

Table 4. Deconvoluted bands peak widths of Raman spectra of silver doped borate glasses

Peak No	B-0	BA-0.25	BA-0.5	BA-0.75	BA-1.0	BA-1.25
1	65	52	46	47	46	57
2	515	535	510	515	573	444
3	175	154	160	157	156	150
4	98	102	102	101	99	106
5	158	139	136	148	162	120
6	365	371	379	354	327	389

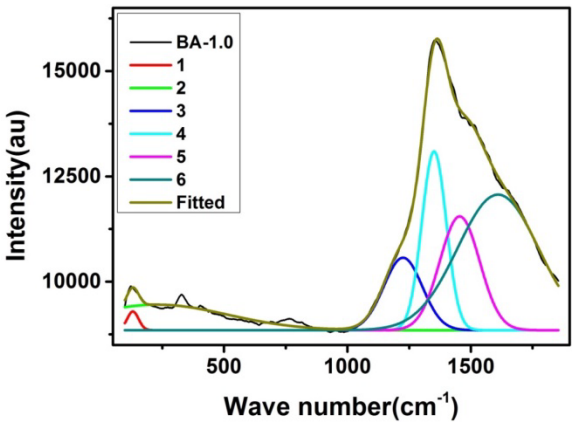

Figure 5. Deconvoluted peaks of the silver doped glasses

Table 5. Deconvoluted bands peak Intensity of Raman spectra of silver doped borate glasses

Peak No	B-0	BA-0.25	BA-0.5	BA-0.75	BA-1.0	BA-1.25
1	423	312	371	418	443	320
2	313	531	483	532	606	517
3	707	1100	1290	1509	1718	1237
4	1594	3306	3821	4103	4243	4487
5	944	1322	1603	2073	2699	1462
6	1386	2809	3538	3390	3219	3965

3.4 UV-Visible studies

Optical properties arise because of the electromagnetic interaction with matter. Nature of the material and the smoothness of the surface, results into different phenomenon. Accordingly the materials may be reflecting (R), transparent (T) or absorbing (A). No substance is perfectly reflecting or perfectly transmitting or perfectly opaque. The sum of the fraction of radiation reflected, transmitted and absorbed is given by R+T+A=1.

3.4.1 UV-Visible absorption

UV-visible absorption spectra of BA- glasses recorded at room temperature are shown in the figure 6. As the wavelength decreased, the absorption very slowly increased and at lower wavelengths the absorption increased drastically. These glasses are transparent to infrared and opaque to ultraviolet light. The absence of sharp band edge indicated the amorphous nature of the material of the glasses. A small absorption band was seen at around 417nm in the silver doped glasses. This band is more intense in BA-1.0 glass. The peak became more prominent with the increase in silver concentration till 1.0mol% and then the band became less intense with further increase in silver content. This band formed due to the collective absorption of silver nano-particles known as band of surface plasmon resonance (SPR). All the silver nanoparticles oscillate in resonance with the incident wavelength.

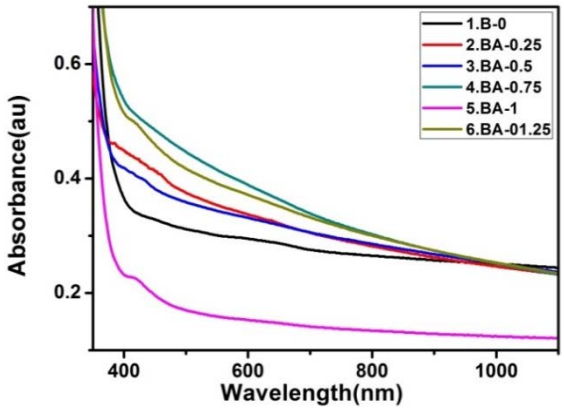

Figure 6. UV-Visible absorption spectra of BA- glasses

The plasmon band indicates the formation of silver nanoparticles which has been explained with the help of SEM and TEM analysis in our further studies in this paper. The peak position changed slightly in the range 414-419nm and the band edge is decreased with the silver addition. SPR peaks at 410nm and 411nm have been reported by previously [20-21]. Similar SPR peaks due to gold nanoparticles were seen in 610–681 nm [22]. At 424nm the SPR band was observed in chitosan mediated silver nanoparticles [23]. SPR band height and the width indicate the number and the size distribution of the nanoparticles. However, for the higher concentration the SPR is found to decrease which may be due to concentration quenching.

3.4.2 Optical band gap energy

The optical absorption edge was found by absorption constant which exponentially rises with energy of photon in amorphous semiconductors.

With the help of the Davis and Mott equation [24] relating the absorption co-efficient and the energy of the e-m waves the optical band gap energies (E_{opt}) of the prepared glasses were determined by the following the formulae.

$$\alpha(\omega) = 2.303\, A/d \tag{3}$$

$$\alpha(\omega) = B\,(h\nu - E_{opt})^n/\hbar\omega \tag{4}$$

where in formula 3, α(ω), the absorption coefficient, A - the absorbance and d - the thickness of the glass and in formula 4, ħω the incident energy, E_{opt} energy difference from the valence to the conduction bands and n is the exponent depends on the inter-band transition mechanism. The values of n may have the values 1/2, 2 for direct allowed and indirect allowed inter band transitions respectively.

The relation between energy and $(\alpha h\nu)2$ and energy against $(\alpha h\nu)^{1/2}$ were plotted as depicted in the figure 7 and figure 8 respectively. The tangents drawn to these curves were extrapolated till $(\alpha h\nu)2 = 0$ and against $(\alpha h\nu)^{1/2}=0$ in the corresponding figures and thus the direct and indirect band gap energies were obtained. The obtained band gap energies with the silver doping are shown in the figure 9. It is found to decrease in the beginning, with silver doping into the base glasses and with further increase in the silver doping the band gap energy increased. But direct band gap energy is always more than the corresponding indirect band gap energy.

The increased in band gap energies depicts that the structure is becoming more open. This may be correlated with the density of the glasses which showed exactly the reciprocal changes with the silver concentration. As the density increases the energy levels spacing decreases and hence there is a decrease in the band gap energy. With the decrease in the density the energy levels will be more spaced and this may be the reason for the increased band gap (Eg) energy. The increasing band edge indicates the non-bridging oxygen formation.

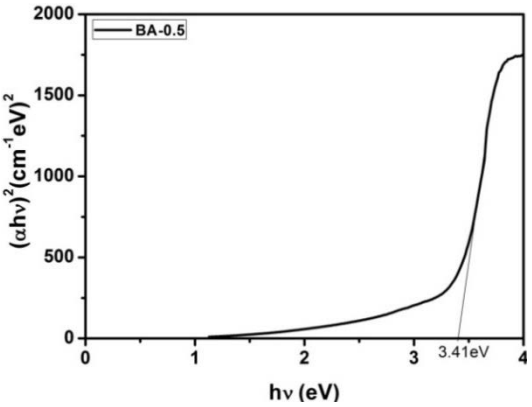

Figure 7. Typical Tauc plots to evaluate the direct band gap energy

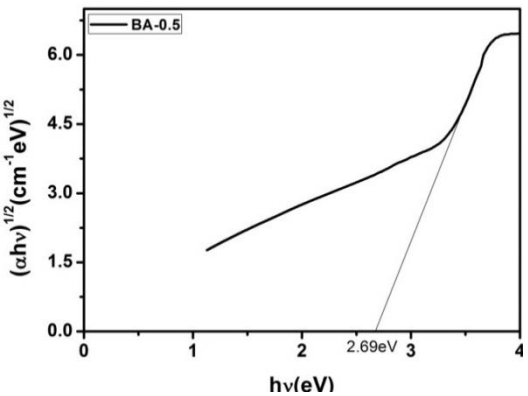

Figure 8. Typical Tauc plot to evaluate the indirect band gap energy

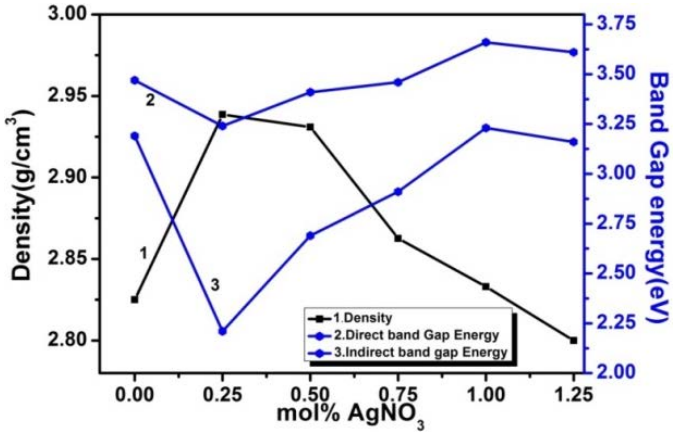

Figure 9. Correlation between the density and band gap energies

3.4.3 Urbach energy

Urbach energy is the measure of disorder which is determined by the UV-Visible absorption data of absorption coefficient and the corresponding energy.

In the exponential region, the shape of the absorption in the tail indicates the disordered nature of the material. In the forbidden band gap, the band edge gives a measure of disorder in the structure of the materials which is evaluated by the use of Urbach rule [25]. The energy against log (α) was plotted to determine the Urbach energy which is 1/ slope of the band edge (Fig. 10). The Urbach energy of these glasses increased initially with silver addition into the matrix and later decreased with further doping of silver which is presented in figure 11. The more the density the more is the disorder observed in the glasses and vice-versa.

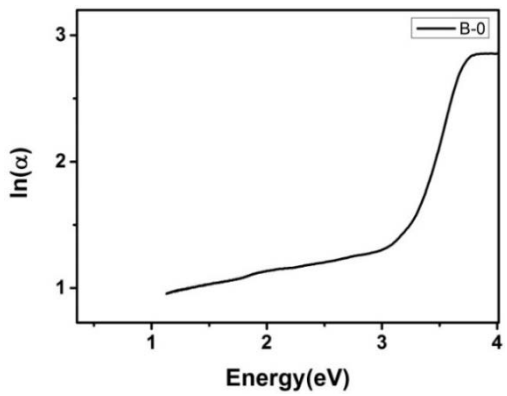

Figure 10. Energy vs. ln [α] plot for the determination of Urbach energy

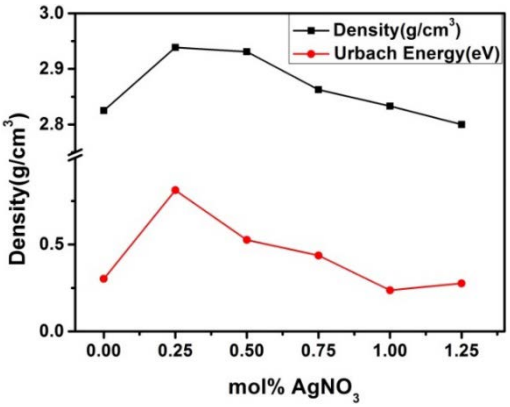

Figure 11. The variation Urbach energy correlated to density with the silver variations

3.5 Particles analysis

3.5.1 Scanning - electron microscopy (SEM)

The Scanning - electron microscope (SEM) was used for the particles morphology. The figure 12 shows the images of the glass samples with scanning electron.

The Ag nano-particles were observed in the BA- glasses. However, in addition to the approximately small spherical nanoparticles, nanowires were also observed. The nanowires were seen in the base glasses also. The nanowires were formed by the matrix of the glass without silver doping. In order to get more clear information of the nanoparticles, transmission electron microscope images were obtained.

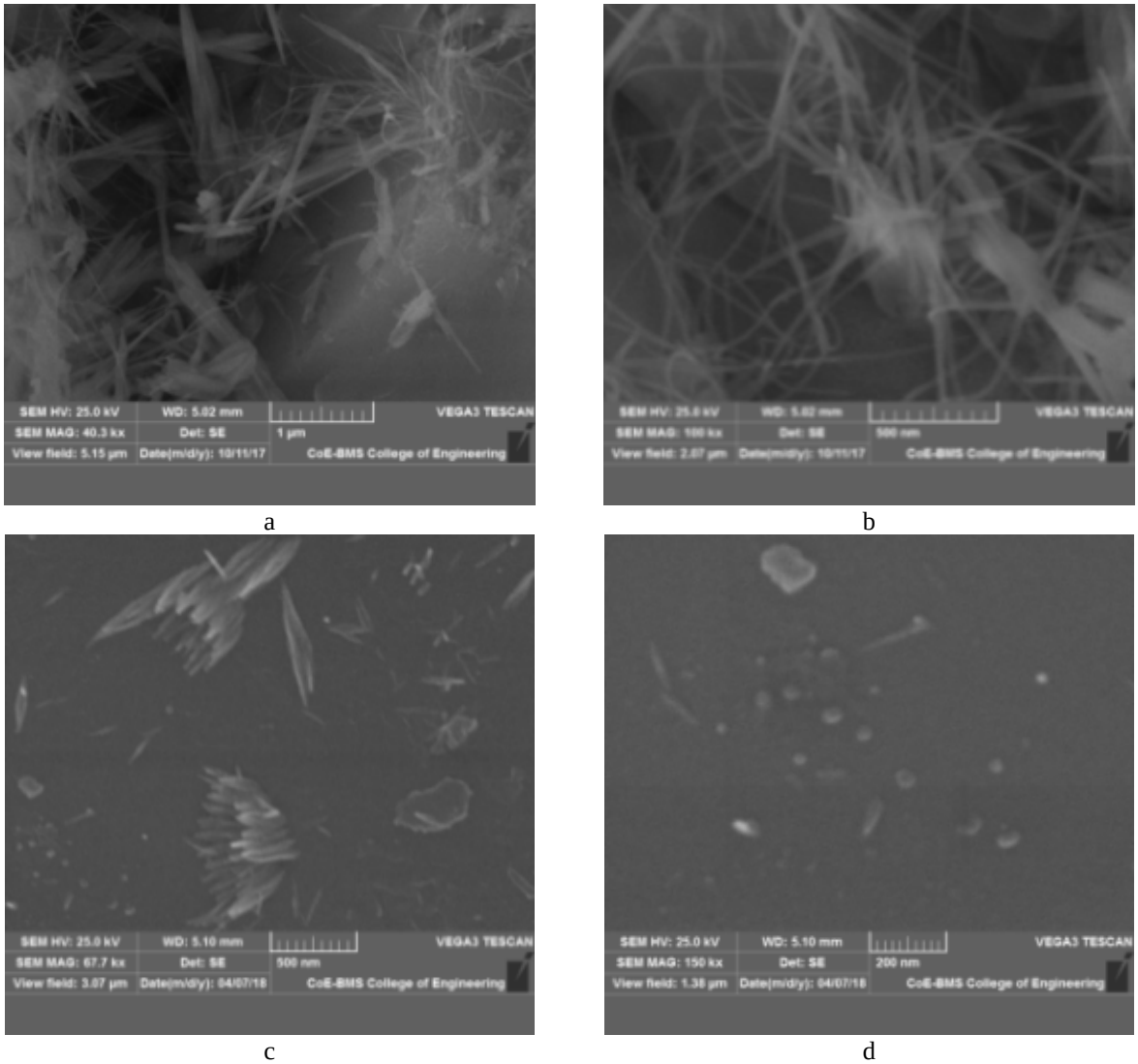

Figure 12. SEM images of base a] and b] and c] and d] BA-1 glasses

3.5.2 Transmission electron microscope (TEM)

These glasses were further examined with transmission electron microscope. It is one of the more significant sophisticated instruments for the analysis of particles. Figure 13a and 13b show the base and the silver doped glasses' TEM images with 10nm and 20nm resolution.

In the B-8 glass without silver, small amount of wire type structures of barium borate nanowires were observed whose average width was around 25nm. Using the surface area electron diffraction (SAED) and the image software they were indexed with the card number 15-860[26 - 28]. In the figure 13c and 13d the silver nanoparticles can be seen with resolution 10 and 20nm.They were further investigated by the SAED and indexed with help of JCPDS card no 65-2871[23]. Silver nanoparticles average size was estimated to be 4nm and identified them as cubic with space group Fm-3m [23].

Electromagnetic (EM) wave whose wavelength, close to the plasmon band if incident on the silver nano-particles, they start to oscillate collectively in resonance is identified as surface plasmon resonance (SPR). Some of the metals, whose conduction electrons readily absorb the EM energy and form surface plasmons are silver, gold and copper etc. These metal nanoparticles serve as sensors and enhance the properties such as luminescence, Raman scattering, electrical properties. The luminescence of the luminescent ions in the vicinity of the silver nanoparticles can be modified by two methods, one through the direct energy transfer from nanoparticles to the ion and other by the electric field enhanced by the surface plasmon.

According to literature this surface plasmon band formed by silver nanoparticles produces luminescence enhancement or luminescence quenching. Our interest was to understand what changes it brings in our barium sodium borate glass with erbium doping so that these glasses may find a place in plasmon application.

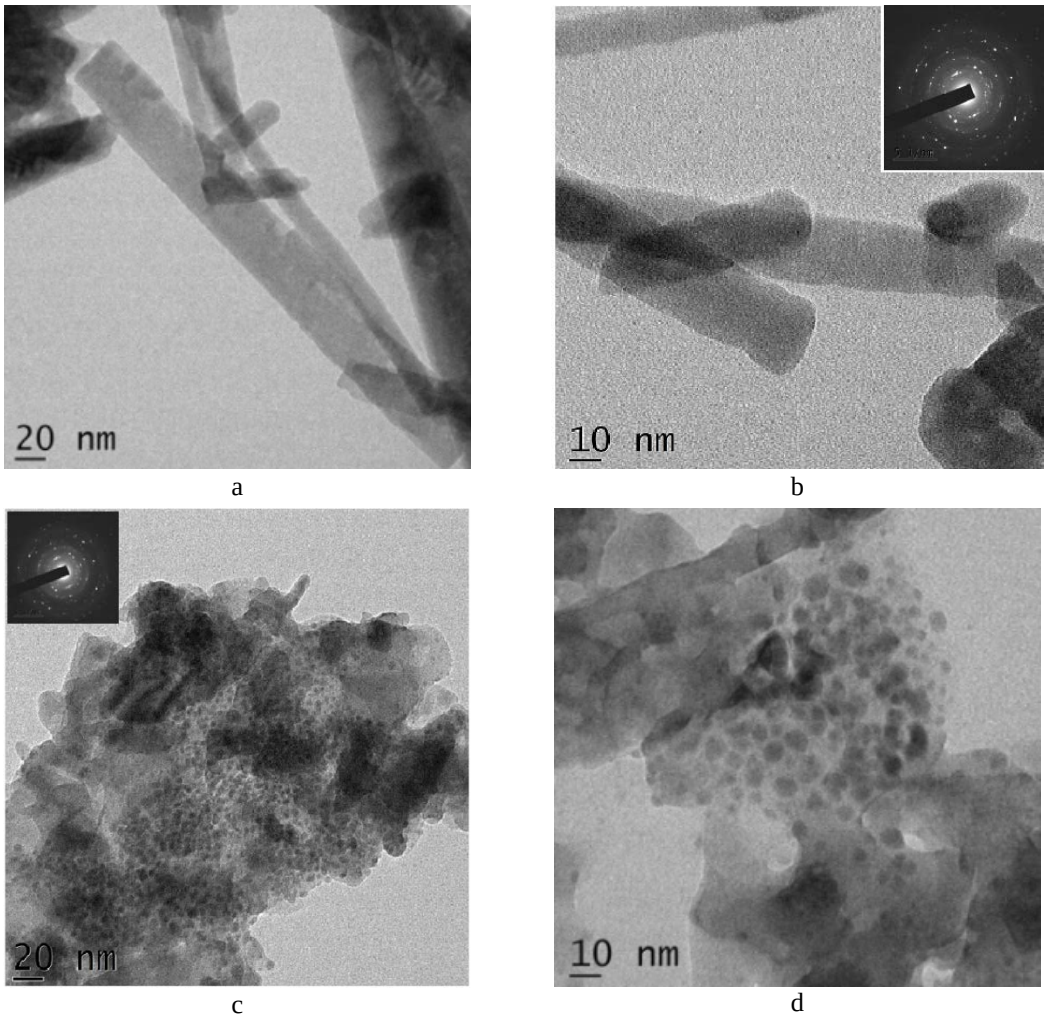

a b

c d

Figure 13. TEM images of a] and b] base & c] and d] BA-1 glasses

3.6 Photoluminescence study

The photoluminescence spectra of the BA-glasses are displayed in the figure 14 for the wavelength excitation of 417nm (Plasmon).

Broad and prominent emission band in the visible region was observed which is the characteristic feature of the silver nanoparticles and is formed due to the SPR of silver nanoparticles. The emission intensity increased with the silver doping and later decreased after 1mol% of silver content. Increase in both width and height of the plasmon band was seen up to 1mol%. In order to compare, the emission spectra of base glass is also shown. Base glass was found to show least intensity without any plasmon resonance band. In the table 6 the emission intensity and emission enhancement of BA glasses are shown. The enhancement increased up to 817 times for 1mol% of silver and thereafter it decreased. All the BA glasses showed increased photoemission.

Photoluminescence spectral data were fed to get CIE (International Commission on Illumination) diagram to perceive the colour of emission. The Co-ordinates of CIE chromaticity of silver doped glasses were found and tabulated in the table 7.

Table 6. The emission intensity enhancement of BA glasses

Glass Code	Silver doping	Emission Intensity	Intensity enhancement
B-0	0	9850	-
BA-0.25	0.25	39640	402
BA-0.5	0.5	56286	571
BA-0.75	0.75	73380	745
BA-1.0	1	80439	817
BA-1.25	1.25	60448	614

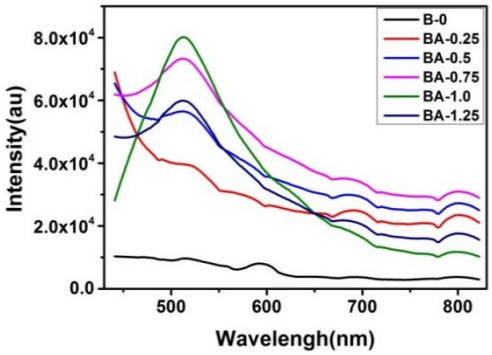

Figure 14. Photoluminescence spectra of silver doped borate glasses

Table 7. CIE co-ordinates and CCT values of the Silver doped glasses

Glass samples	Colour Co-ordinates		
	x	y	CCT
B-0	0.3	0.36	6896
BA-0.25	0.3	0.39	6678
BA-0.5	0.31	0.36	6438
BA-0.75	0.31	0.39	6295
BA-1.0	0.3	0.41	6567
BA-1.25	0.3	0.39	6678

The temperature of the colour emitted proposed by Planckian black body known as the correlated colour temperature (CCT) were also determined and are shown in the table 7. For understanding the emission colour quality the Empirical McCamy equation [29-32] was used.

$$\mathrm{CCT} = -449n^3 + 3525n^2 - 6823\mathrm{n} + 5520.33 \quad (5)$$

where n=[x-xc]/[y-yc] and the chromaticity epi centre (xe, ye) = (0.32 0.1858) [33]. The mean CCT obtained was 6531K.

The CCT values less than 4000 emitted the apparent warm colours consisting of more red and yellow colours used for dim lighting. The CCT values greater and equal 4000 emitted the apparent cool colours consisting of more crisp white or blue light used for more sophisticated applications. All the glasses displayed the emission in the green and blue portion of electro-magnetic radiation very near proximity of white light with varying intensity and highest being for BA-1 glass.

The silver nanoparticles collectively oscillated when excited by the plasmon wavelength and gave a broad emission in the visible region very close to white light as shown in the figure 15. This broad luminescence band may be used to enhance the luminescence of rare earth ions [36]. The energy of emission of all of the silver nanoparticles when plasmon excited oscillate together and may transfer the energy directly to the nearby emission centers like rare earth ions or this collective oscillation may produce the high electric field which may also excite the rare earth ions and help in improving the emission of rare earth ions [34-37]. This plasmonic phenomenon can be used in enhancing the luminescence of the rare earth ions which used in the LED applications.

4. Conclusion

Sodium-Barium-Borate glasses tamper with silver nano-particles were successfully synthesized by the melt-quenching practice with different silver concentrations. The Amorphous behaviour of glasses was understood by the lack of clear and distinct peaks in the XRD. The FTIR and Raman studies revealed the presence of BO3 and

BO4 units. In the UV-Visible absorption studies, formation of silver nanoparticles was confirmed by the appearance of plasmon band. Further size, shape and the distribution of nanoparticles were understood by the SEM and TEM analysis. The band gap energies and Urbach energies were found to vary with the density of the glasses indirectly and directly respectively. A broad emission band was witnessed due to the plasmon resonance of the silver nanoparticles, for the excitation wavelength of plasmon peak. This broad emission of silver nanoparticles may be harnessed to enhance the rare earth emission in the visible region.

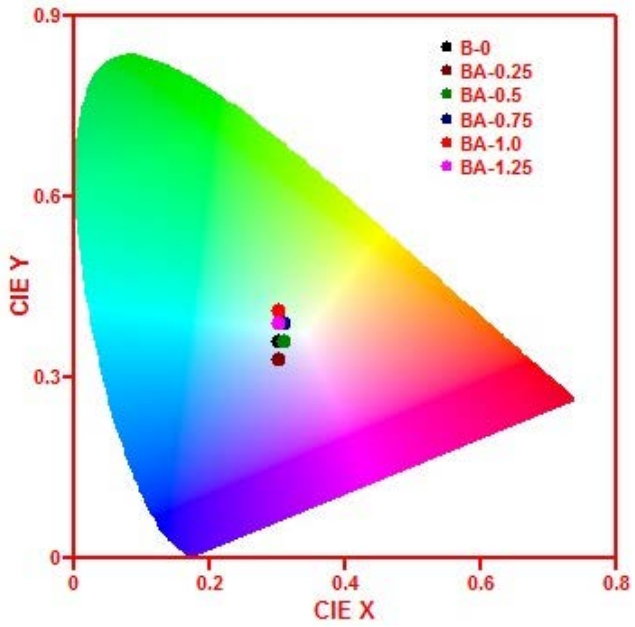

Figure 15. CIE-diagram showing the emission colour of silver doped glasses

5. Acknowledgments

The author Rajeshree Patwari D. expresses her sincere gratitude to University Grants Commission for providing FDP fellowship to carry out the research work.

6. References

[1] Ota R, Yasuda T, Fukunaga J. Structure of alkali borate glasses based on the chemical equilibrium concept. Journal of Non-Crystalline Solids. 1990;116: 46-56.
[2] Jiao Q, Li G, Zhou D, Qiu J. Effect of the glass structure on emission of rare-earth-doped borate glasses. Journal of the American Ceramic Society. 2015; 98(12): 4102–4106.
[3] Shaaban KHS, Saddeek YB, Sayed MA, Yahia IS. Mechanical and thermal properties of lead borate glasses containing CaO and NaF. Silicon. 2018; 10:1973–1978.
[4] Thakur V, Singh A, Punia R, Dahiya S, Singh L. Structural properties and electrical transport characteristics of modified lithium borate glass ceramics. Journal of Alloys and Compounds. 2017; 696:529-537.
[5] Ivanova OS, Ivantsov RD, Edelman IS, Petrakovskaja EA, Velikanov DA, Zubavichus YV, Zaikovskii VI, Stepanov SA. Identification of ε-Fe_2O_3 nano-phase in borate glasses doped with Fe and Gd. Journal of Magnetism and Magnetic Materials. 2016; 401: 880-889.
[6] Bengisu M. Borate glasses for scientific and industrial applications: a review. Journal of Materials Science. 2016; 51: 2199–2242.
[7] Pisarski WA, Goryczka T, Wodecka-Duś B, Płońska M, Pisarska J. Structure and properties of rare earth-doped lead borate glasses. Materials Science and Engineering B. 2005; 122:94–99.
[8] Souto S, Massot M, Balkanski M, Royer D. Density and ultrasonic velocities in fast ionic conductingborate glasses. Materials Science and Engineering: B. 1999; 64(1): 33–38.
[9] Souza Filho AG, Mendes Filho J, Melo FE, Custodio MC, Lebullenger R, Hernandes AC. Optical properties of Sm3+ doped lead fluoroborate glasses. Journal of Physics and Chemistry of Solids. 2000; 61:1535–1542.
[10] Datta S, Bahadur D, Chakravorty D. Magnetic properties of barium borate glasses containing nickel micro-granules. Journal of Physics D: Applied Physics. 1984; 17: 163-169.

[11] Reza Dousti M, Sahar MR, Ghoshal SK, Raja J, Amjad R. Plasmonic enhanced luminescence in Er3+: Ag co-doped tellurite glass. Journal of Molecular Structure. 2013; 1033:79–83.
[12] Muhammad Noorazlan A, Kamari HM, Omar Baki S, Mohamad DW. Green emission of tellurite based glass containing erbium oxide nanoparticles. Journal of Nanomaterials. 2015; 2015: 952308.
[13] Motke SG, Yawale SP, Yawale SS. Infrared spectra of zinc doped lead borate glasses. Bulletin of Materials Science. 2002;25(1):75-78.
[14] Gautam CR, Yadav AK. Synthesis and optical investigations on (Ba,Sr)TiO3 borosilicate glasses doped with La2O3. Optics and Photonics Journal. 2013; 3: 1-7.
[15] Gautam C, Yadav AK, Singh AKA. Review on infrared spectroscopy of borate glasses with effects of different additives. ISRN Ceramics. 2012; 2012: 428-497.
[16] Padmaja G, Kistaiah P. Infrared and Raman spectroscopic studies on alkali borate glasses: Evidence of mixed alkali effect. The Journal of Physical Chemistry A. 2009; 113(11): 2397–2404.
[17] Kamitsos EI, Karakassides MA, Chryssikos GD. Vibrational spectra of magnesium-sodium- borate glasses. 2. Raman and mid-infrared investigation of the network structure. The Journal of Physical Chemistry. 1987; 91: 1073-1079.
[18] Markova TS, Yanush OV, Polyakova IG, Pevzner BZ, Klyuev VP. Structure–property relations in barium borate glasses from Raman scattering data. Glass Physics and Chemistry.2005; 31(6):721–733.
[19] Konijnendltk WL,Verweij H. Structural aspects of vitreous pb0.2b203 studied by Raman scattering. Journal of the American Ceramic Society. 1976; 59(9-10): 459–461.
[20] Qi J, Xu T, Wu Y, Shen X, Dai S, Xu Y. Ag nanoparticles enhanced near-IR emission from Er3+ ions doped Glasses. Optical Materials. 2013; 35: 2502–2506.
[21] Vijayakumar R, Nagaraj R, Suthanthirakumar P, Karthikeyan P, Marimuthu K. Silver (Ag) nanoparticles enhanced luminescence properties of Dy3+ ions in borotellurite glasses for white light applications. Spectrochimica Acta Part A: Molecular and Biomolecular Spectroscopy.2018; 204: 537-547.
[22] Som T, Karmakar B. Surface plasmon resonance and enhanced fluorescence application of single-step synthesized elliptical nano gold-embedded antimony glass dichroic nanocomposites. Plasmonics. 2010; 5:149–159.
[23] Kalaivani R, Maruthupandy M, Muneeswaran T, Hameedha Beevi A, Anand M, Ramakritinan CM, Kumaraguru AK. Synthesis of chitosan mediated silver nanoparticles (Ag NPs) for potential antimicrobial applications. Frontiers in Laboratory Medicine. 2018; 2: 30-35.
[24] Davis EA, Mott NF. Conduction in non-crystalline systems V. Conductivity, optical absorption and photoconductivity in amorphous semiconductors. Philosophical Magazine. 1970; 22(179): 0903-0922.
[25] El-Rabaie S, Taha TA, Higazy AA. Compositional dependence thermal and optical properties of a novel germanate glass. Physica B: Condensed Matter. 2014; 432:40–44.
[26] Zhao Q, Zhu X, Bai X, Fan H, Xie Y. Synthesis and optical properties of β-BaB2O4 network-like nanostructures. European Journal of Inorganic Chemistry.2007; 13:1829–1834.
[27] Qu G, Hu Z, Wang Y, Yang Q, Tong L. Synthesis of optical-quality single-crystalβ-BaB_2O_4 microwires and nanowires. Advanced Functional Materials. 2012; 23(10): 1232–1237.
[28] Lopes AAS, Monteiro RCC, Soares RS, Lima MMRA, Fernandes M.H.V. Crystallization kinetics of a barium–zinc borosilicate glass by a non-isothermal method. Journal of Alloys and Compounds.2014; 591: 268–274.
[29] McCamy CS. Correlated color temperature as an explicit function of chromaticity coordinates. Color Research & Application.1992; 17(2):142–144.
[30] Deopa N, Rao AS. Photoluminescence and energy transfer studies of Dy 3+ ions doped lithium lead alumino borate glasses for w-LED and laser applications. Journal of Luminescence. 2017; 192: 832–841.
[31] Ramachari D, Moorthy LR, Jayasankar CK. Energy transfer and photoluminescence properties of Dy3+/Tb3+ co-doped oxyfluorosilicate glass–ceramics for solid-state white lighting. Ceramics International. 2014; 40(7): 11115–11121.
[32] Rekha Rani P, Venkateswarlu M, Mahamuda SK, Swapna K, Deopa N, Rao AS. Spectroscopic studies of Dy3þ ions doped barium lead alumino fluoro borate glasses. Journal of Alloys and Compounds. 2019; 787: 503-518.
[33] Hernández-Andrés J, Lee RL, Romero J. Calculating correlated color temperatures across the entire gamut of daylight and skylight chromaticities. Applied Optics. 1999; 38(27): 5703-5709.
[34] Fares H, Elhouichet H, Gelloz B, Férid M. Silver nanoparticles enhanced luminescence properties of Er3+ doped tellurite glasses: Effect of heat treatment. Journal of Applied Physics. 2014;116(12): 123504-123513.
[35] Amjad RJ, Sahar MR, Ghoshal SK, Dousti MR, Samavati AR, Riaz S, Tahir BA. Spectroscopic investigation of rare-earth doped phosphate glasses containing silver nanoparticles. Acta Physica Polonica A. 2013; 123(4): 746–749.

[36] Ashur Z, Sahar MR., Ghoshal SK, Dousti MR, Amjad RJ. Silver nanoparticles enhanced luminescence of Er3+ ions in boro-tellurite glasses. Materials Letters. 2013; 112: 136–138.
[37] Soltani I, Hraiech S, Horchani-Naifer K, Elhouichet H, Férid M. Effect of silver nanoparticles on spectroscopic properties of Er3+ doped phosphate glass. Optical Materials. 2015; 46: 454–460.